CH···F Hydrogen Bonds. Dimers of Fluoromethanes

Eugene Kryachko† and Steve Scheiner*

Departement de Chimie B6c, Universite de Liege, Sart-Tilman, B-4000 Liege 1, Belgium, Bogoliubov Institute for Theoretical Physics, Kiev, 03143 Ukraine, and Department of Chemistry & Biochemistry, Utah State University, Logan, Utah 84322-0300

Received: August 22, 2003; In Final Form: December 3, 2003

The nature of the CH···F H-bond is studied by examining the potential energy surfaces for dimers of the fluoromethanes, including all homo- and heterodimers involving CH_4, CFH_3, CF_2H_2, CF_3H, and CF_4. Several of the surfaces encompass two separate minima. Any pair capable of forming a cyclic structure does so, this geometry being more stable than any other minima that might occur on the surface. Such cyclic dimers are bound by 2−3 kcal/mol. Noncyclic geometries are only very weakly bound. In all cases, the C−H bonds that participate directly in the H-bonds undergo a contraction and associated blue shift in their stretching frequencies, whereas the C−F bonds manifest an elongation. The most strongly bound of all dimers studied pairs CH_3F with CHF_3, for which the C−H bond contracts by 0.0023 Å, and its stretching frequency increases by 39 cm^{-1}. The most stable cyclic dimer of fluoroform, containing one single and one bifurcated hydrogen bond, is reported for the first time and thus resolves the longstanding problem of the structure of the fluoroform dimer.

Introduction

Since the general AH···B hydrogen bond concept was originally proposed, there has been a continuing debate about the ability of fluorine to act as an acceptor atom in the B molecule, and how strong such AH···F interactions might be, especially in comparison to the more traditional AH···O and AH···N varieties.[1−7] Likewise, the possibility of a H-bond in which CH acts as donor has been the subject of active discussion. The ability of fluorocarbons such as fluoroform, for example, to form a H-bond has a long history of inquiry.[8−19] A consensus is emerging that such CH···B bonds are indeed possible, particularly if the CH is "activated" by the proximity of electronegative groups that help strengthen its acidity.[6,20−26]

We concern ourselves here with an inquiry into the nature of the interaction that occurs when the two are combined. That is, can a CH donor form a H-bond with a F acceptor, and if so, what sort of strength might be anticipated? There have been several "sightings" of such interactions in crystals[27−31] but it is difficult to determine whether the CH and F groups are truly attracted to one another or are thrust together by other constraints placed on the crystal structure. The recent findings of particularly short CH···FC interaction, wherein the H and F are separated by only 2.20−2.26 Å,[32,33] adds fuel to the idea that such an interaction may indeed be attractive. Some theoretical studies have addressed this issue,[12,34,35] but not in any comprehensive fashion. CH···F bonds have also been of interest recently in a biological context, e.g., their possible presence in nucleic acid derivatives.[36−40]

To examine this question systematically, we consider here the full range of fluoromethanes, beginning with unsubstituted CH_4, then adding F atoms one at a time, up to CF_4. These molecules are then paired together in all combinations. The potential energy surface of each pair is searched for all minima, global and local. The results are analyzed for evidence of CH···F H-bonds of various types, as well as the depth of the minima and energetics of interconversion. Of particular interest are any changes in the internal geometries of each monomer that are associated with formation of the complex.

From a more fundamental perspective, it was thought until only very recently that all H-bonds (XH···Y) were characterized by a red shift in the stretching frequency of the covalent X−H bond. However, recent work has revealed a surprising new class of H-bonds, most of the CH···O or CH···N type, in which the CH stretching frequency shifts in the opposite direction.[10,13,16,22,25,41−44] Such "blue-shifting" H-bonds have engendered a number of studies intended to understand the source of this contrary behavior.[15,19,26,45−50] It is natural then to inquire as to whether the replacement of the O and N proton acceptors by F might likewise lead to a blue shift of the C−H bond. The dimers of fluoromethanes studied in this work can be considered to play the same role in the context of blue-shifting H-bonds, as does the archetypal water dimer in the theory of conventional, red-shifted hydrogen bonds, and their study is thus both natural and timely.

Computational Methodology

All calculations were performed using the *GAUSSIAN 98* suite of programs.[51] The second-order perturbation Møller−Plesset method (MP2), including the frozen core approximation (fc), was used to assess electron correlation. Some key structures were further refined within the MP2(full) context. The 6-31+G-(d,p) basis set was employed to conduct the tight geometry optimizations of all studied dimers and to calculate their harmonic vibrational frequencies and unscaled zero-point vibrational energies (ZPVE). Basis-set superposition errors (BSSEs) were estimated and corrected for all structures via the

* Corresponding author. Utah State University. E-mail: scheiner@cc.usu.edu.

† Universite de Liege and Bogoliubov Institute for Theoretical Physics. E-mail: eugene.kryachko@ulg.ac.be.

10.1021/jp0365108 CCC: $27.50
Published on Web 03/09/2004

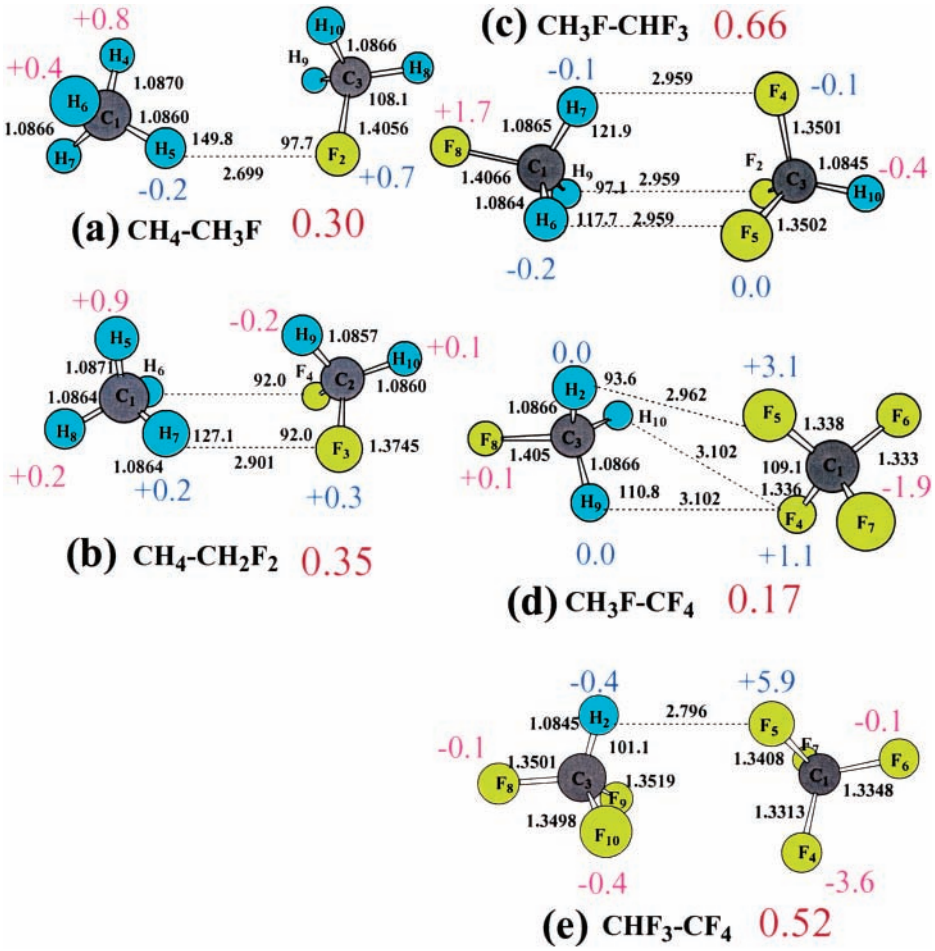

Figure 1. Geometrical configurations of D complexes of fluorocarbon dimers. Large red numbers indicate BSSE-corrected binding energies (kcal/mol). Changes in internal bond lengths arising from complexation are shown by blue and magenta numbers near pertinent atom (in milliangstroms). Bond lengths are reported in angstroms and bond angles in degrees.

counterpoise method implemented in *GAUSSIAN 98*. NBO analysis was also conducted for certain representative structures.

Results

Classification and General Energetic Features. The structures of all of the complexes can be divided into two general categories. In cases where more than one CH···F bond is present, one of the molecules can act as proton donor in all such bonds, and the other as multiple acceptor. These complexes, illustrated in Figures 1 and 2, will be referred to as "D" to indicate their "solely donor" characteristic. Some of the D-type structures do not have a simple CH···F interaction as such, but rather two (or more) hydrogens act as bridge in some of these complexes. The D-type structures can be further partitioned into the following subcategories: (i) a simple CH···F interaction; (ii) bifurcated interaction; (iii) trifurcated interaction. Structures belonging to (i) are displayed in Figure 1, with the unique exception of **1d**, which contains elements of both (i) and (ii). Complexes belonging to subcategories (ii) and (iii) are gathered together in Figure 2, wherein all structures belong to (ii), with the exception of the trifurcated bonds in **2e** and **2f**, placing them in subcategory (iii). It should be noted at the outset that the H···F contact distances of many of the complexes displayed in Figures 1 and 2 are longer than the sum of van der Waals radii of H and F (2.76 Å). These long distances represent an argument against the classification of each as a legitimate H-bond.

The aforementioned D complexes are distinguished from those "DA" complexes depicted in Figure 3 wherein each molecule acts simultaneously as both donor and acceptor. Such structures are commonly alternately referenced as "cyclic". It should be stressed that the above designations are loose ones, designed to place what may be complicated geometries into one category or another. Certain dimers may contain elements of more than one classification. One of the $(CH_2F_2)_2$ dimers in Figure 3, for example, is classified as DA in that each molecule acts as both proton donor and acceptor, but the CH···F interactions are bifurcated as well.

In addition to some of the salient geometrical parameters that are reported for each geometry in Figures 1−3, the large red numbers indicate the computed binding energies in kcal/mol, after correction for basis set superposition error. There are certain patterns that are apparent. The binding energies of the D nonbifurcated H-bonded dimers in Figure 1 fall into the 0.2−0.7 kcal/mol range. The increase in the number of CH···F bonds from 1 to 2 associated with the change from CH_4···CH_3F to CH_4···CH_2F_2 raises the total interaction energy very little, from 0.30 to 0.35 kcal/mol. A slightly larger increment occurs when a F atom is added to the donor molecule, as in CH_3F···CHF_3 (0.66 kcal/mol), although such arguments are oversimplified.

It is interesting to consider these patterns of energetics in terms of any charge transfer that occurs upon formation of a hydrogen bond (see ref 50 and references therein). In **1a**, for example, such electron transfer is observed from the accepting C_3-F_2 bond to the antibonding σ_{CH}* molecular orbital (MO) of the proton donor. Specifically, F_2 loses 0.004 e (Mulliken charge) whereas H_5 picks up an additional 0.017 e. This loss of

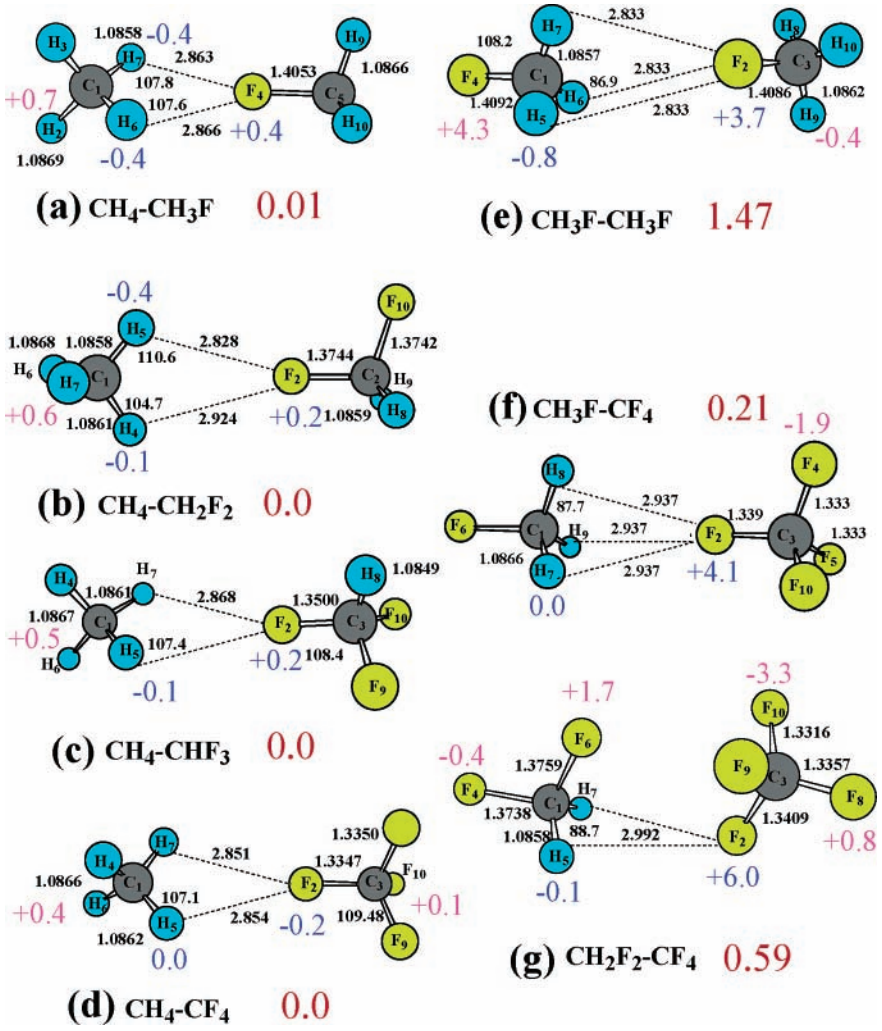

Figure 2. Geometrical configurations of D complexes containing bifurcated or trifurcated H-bonds.

density on F_2 may help account for the elongation of the C_3-F_2 bond by 0.7 mÅ (shown in blue in Figure 1), and the presumable accompanying bond weakening. The arguments described in ref 50 would consider the short $H_5\cdots F_2$ distance of 2.699 Å in **1a** as a suggestion that rehybridization is favored over hyperconjugation. The $CH_4\cdots CH_2F_2$ complex in **1b** contains two parallel H-bonds. The simultaneous charge transfers to σ_{CH}* of methane from the C_2-F_3 and C_2-F_4 bonds result in additional electron density accumulation on H_6 and H_7 of 0.006 e, less than the 0.017 e in **1a**. The division of the charge transfer into two separate H-bonds in **1b** may thus account for the longer $F_3\cdots H_7$ and $F_4\cdots H_6$ distances (2.901 Å), and lesser elongation of the C−F bonds of CH_2F_2, compared to **1a**. Similar arguments apply to **1c** where the charge transferred along each of the three hydrogen bonds is considerably reduced. In the $CH_3F\cdots CHF_3$ case, however, the binding energy profits from the nearly perfect collinear alignment of the dipole moments of the constituting molecules, and the accompanying stabilizing dipole−dipole interaction.

The bi- and trifurcated interactions illustrated in Figure 2 are considerably weaker. Indeed, most of these have binding energies very close to zero. The prime exception is the trifurcated C_{3v} homodimer of CH_3F (**2e**) with a binding energy of 1.47 kcal/mol. However, it is likely that this interaction is due largely to a favorable alignment of the two molecular dipoles, rather than a strong CH···F interaction per se. (It might be worth noting that the B3LYP/6-311++G(3df,3pd) method yields longer intermolecular distances, e.g., $R(F_2-H_{5-7}) = 2.99$ Å vs 2.833 Å, and a weaker binding energy of 0.93 kcal/mol.[52]) The bifurcated arrangements are hence considered the weakest of the interaction types, which may be connected to the mutual Coulomb repulsion of the partial charges transferred from proton acceptor to donor upon formation of the H-bond.

Indeed, this very same CH_3F dimer has a second minimum, of lower energy, on its potential energy surface. The global minimum, illustrated in Figure 3a, is of DA, or cyclic type, of C_{2v} symmetry. (A B3LYP/6-311++G(3df,3pd) calculation[52] yielded a similar equilibrium structure, with a binding energy of 1.55 kcal/mol.) Even though the two molecular dipoles are antiparallel, this structure is still bound more strongly than is the trifurcated geometry in Figure 2e. In fact, it is the DA type of geometry that is generally most stable. Interaction energies vary from 1.6 to 2.8 kcal/mol, the latter for $CH_3F\cdots CHF_3$. Note that this particular structure is far more stable than the D geometry of the same complex (0.66 kcal/mol), depicted in Figure 1c. This overall preference for DA structure may be taken as one manifestation of the positive cooperativity that can be realized in such an arrangement.

Regarding the relative strengths of the various DA complexes in Figure 3, there does appear to be some preference for different degrees of fluorosubstitution in the two subunits. For example, the most strongly bound complex is $CH_3F\cdots CHF_3$ which contains three F atoms on one molecule and only one on the other, and the weakest, $CHF_3\cdots CHF_3$, has the same number (three) F atoms on both subunits. Between these two extremes,

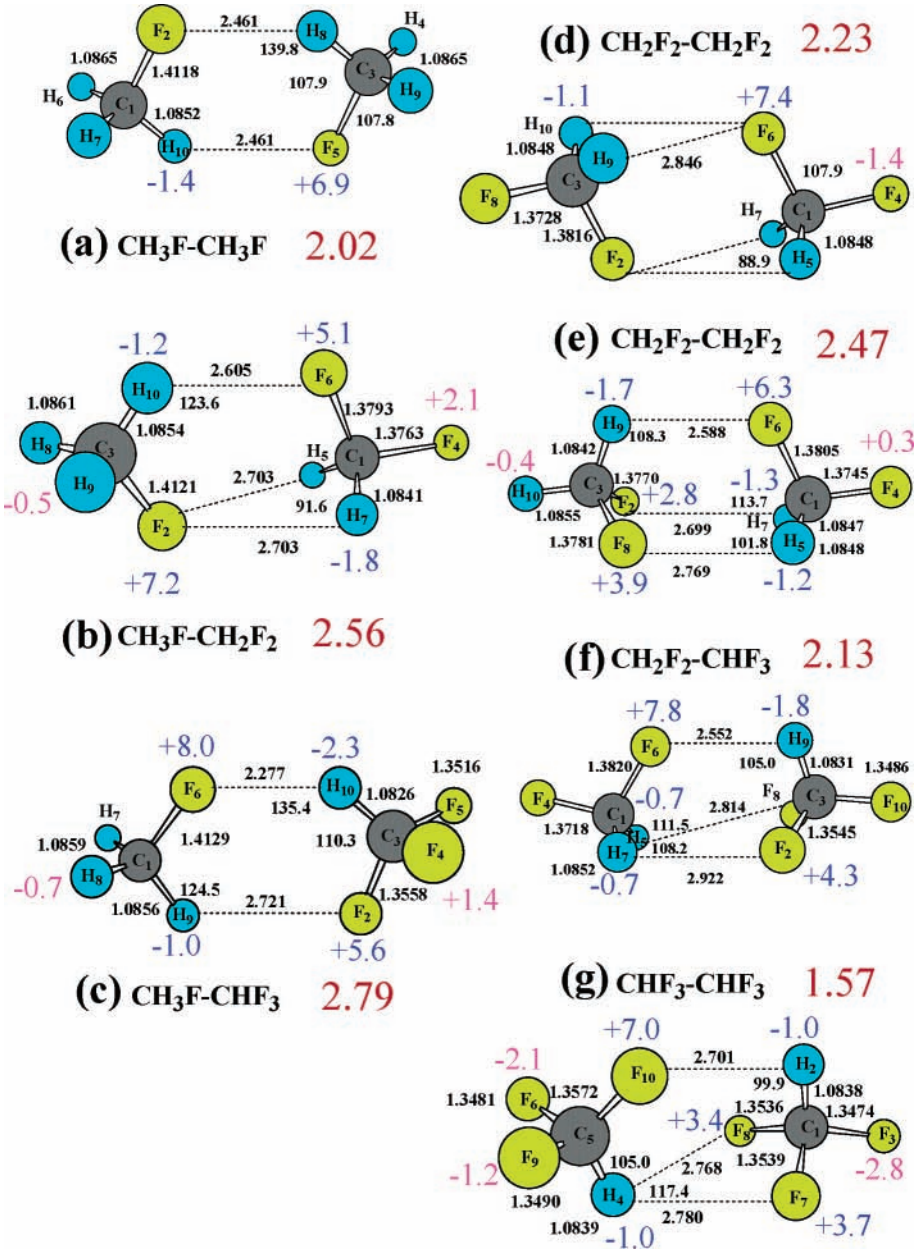

Figure 3. Geometrical configurations of cyclic DA complexes in which each molecule acts simultaneously as proton donor and acceptor.

the second most strongly bound cyclic dimer $CH_3F\cdots CH_2F_2$ exceeds the "equisubstituted" $CH_2F_2\cdots CH_2F_2$ and $CH_3F\cdots CH_3F$.

One can understand some of the relative H-bond strengths on the basis of the electronegativity of the F atoms. The presence of three electron-withdrawing F atoms on CHF_3 would tend to make its H most acidic. Indeed, the deprotonation energy of this molecule is the smallest of this group of fluoromethanes.[53−55] Likewise, the single F atom in CH_3F might be expected from first principles to make this atom the best proton-acceptor. It is hence not surprising that the H-bond pairing the H of CHF_3 with the F of CH_3F in complex **3c** makes for the shortest (2.277 Å at MP2(fc) and 2.275 Å at MP2(full)), and presumably strongest, H-bond of all those considered here. This contention of H-bond energy is supported by the fact that this same complex is most strongly bound, despite the rather long (2.721 Å at MP2(fc) and 2.710 Å at MP2(full)) character of the other H-bond in **3c**. (It must be noted, however, that the proton affinity of CH_3F is surprisingly small when calculated, only 143.1 kcal/mol, as compared to 148.3 and 148.1 kcal/mol for CH_2F_2 and CHF_3, respectively. This observation underscores the point that the proton affinity of a given molecule is only one of several properties that must be considered in predicting H-bond strengths.)

For purposes of comparison, the rotational constants of all of our minima are reported in Table 1, along with the experimental data available for the CH_2F_2 dimer.[56,57] Also listed are the distances separating the central carbon atoms in each complex. Perusal of these data indicates that the intercarbon distances for the structures in Figure 1 vary between 3.66 and 3.96 Å, but there is no clear relation between this distance and binding energy. These same intermolecular distances are longer, in the 3.91−4.76 Å range, for the bifurcated geometries in Figure 2. The shortest separations are associated with the strongest complexes, the DA configurations in Figure 3, where R(C···C) varies between 3.52 and 3.92 Å. It might be noted, however, that despite their considerably greater binding energies, the latter DA complexes have separations only slightly shorter than those with a simple CH···F interaction (**1a** and **1e**) in Figure 1, which suggests their cyclic geometries tend to hold the C atoms a little further apart.

TABLE 1: Rotational Constants of the Fluoromethane Dimers Calculated at the MP2(fc)/6-31+G(d,p) Computational Level, Intercarbon Separation (Å), and Binding Energy (kcal/mol) Corrected for BSSE and ZPVE

		A, MHz	*B*, MHz	*C*, MHz	*R*(C···C), Å	E_d,[a] kcal/mol
$CH_4\cdots CH_3F$	**1a**	22178.34	3192.99	2893.26	3.920	0.16
	2a	79221.60	2549.08	2548.88	4.762	0.31
$CH_4\cdots CH_2F_2$	**1b**	8588.85	3055.93	2476.14	3.659	0.18
	2b	22962.36	1776.07	1684.43	4.741	0.37
$CH_4\cdots CHF_3$	**2c**	9195.54	1532.26	1369.085	4.704	0.37
$CH_4\cdots CF_4$	**2d**	5407.73	1296.90	1296.89	4.674	0.40
$CH_3F\cdots CH_3F$	**3a**	12788.01	2554.24	2188.40	3.875	−1.36
	2e	78460.24	1374.59	1374.59	4.386	−1.20
$CH_3F\cdots CH_2F_2$	**3b**	11916.84	1628.88	1460.19	3.746	−1.95
$CH_3F\cdots CHF_3$	**3c**	5635.31	1293.38	1278.28	3.919	−2.30
	1c	5379.15	1103.84	1103.11	3.746	−0.39
$CH_3F\cdots CF_4$	**1d**	5375.31	776.39	775.79	3.961	0.07
	2f	5405.17	657.52	657.52	4.429	−0.04
$CH_2F_2\cdots CH_2F_2$	**3e**	6322.23	1311.68	1253.99	3.524	−1.89
exp[56]		6447.7(22)	1290.238(8)	1234.614(10)	3.542(7)	
exp[57]		6465.38(37)	1290.36829(65)	1234.39416(62)		
	3d	12463.64	971.59	912.22	3.650	−1.74
$CH_2F_2\cdots CHF_3$	**3f**	6483.79	889.24	863.57	3.569	−1.67
$CH_2F_2\cdots CF_4$	**2g**	4696.87	736.71	722.11	3.905	−0.27
$CHF_3\cdots CHF_3$	**3g**	4211.35	783.89	717.73	3.638	−1.22
$CHF_3\cdots CF_4$	**1e**	3507.26	664.84	633.77	3.889	−0.22

[a] Negative values correspond to bound states, and positive to situations where isolated monomers lie lower in energy than complex.

The final column of Table 1 reports the binding energy of each complex, following correction for both basis set superposition error and zero-point vibrational energy. Note that some of these quantities are positive, which indicates the energy of the complex is higher than that of the separated monomers (within the employed scheme of correcting the basis set superposition error and using unscaled harmonic vibrational frequencies).

Complexes Involving CH_4. The unfluorinated methane molecule offers only very weak interactions. The optimized geometries are all of the bifurcated variety, illustrated by the left side of Figure 2, and are scarcely bound at all, particularly after basis set superposition is corrected. Indeed, addition of zero-point vibrational energies raises the energies of these complexes above those of their separated substituents (see Table 1). On the other hand, the pairing of methane with CH_3F and CH_2F_2 yields a second, and more stable, minimum. As depicted on the left side of Figure 1, these interactions contain nonbifurcated CH···F bonds, although the CH···F angles deviate considerably from the idealized value of 180°. On the other hand, such deviations are not unusual for bonds of this type. For instance, a recent calculation of the $HOH\cdots FCH_3$ complex[58] found optimized C−F···O and F···H−O angles of 90° and 144°, respectively, at equilibrium C···O and F···H distances of 3.254 and 2.117 Å. These geometrical details were in close correspondence with X-ray data dealing with the C−F···H hydrogen bonds reported by Murray-Rust et al.,[2] an agreement which Monat et al. termed "accidental" because there are other, stronger, interactions present in the crystals. It may be that this coincidence is not accidental, and that such "misalignment" makes for effective overlap between molecular orbitals of CH_3F and H_2O. Indeed, this notion is further buttressed by another survey of crystal data,[3] which had concluded that the CH···F angle typically lies in the range between 130° and 145°.

Though slightly stronger than their bifurcated secondary minima, the interaction energies of these nonbifurcated structures are only on the order of 0.3 kcal/mol and vanish if (unscaled harmonic) ZPVE is included. The secondary minima can be exceedingly shallow. For example, the transition state for the conversion of structure **2a** of $CH_4\cdots CH_3F$ to the more stable **1a** involves a barrier of only 0.03 kcal/mol. In summary, one would not expect complexes involving CH_4 to be easily detectable.

Complexes Involving CH_3F. Adding even a single electron-withdrawing F atom to methane strengthens its proton-donating ability to the point where complexes ought to be observable. As an interesting prelude to this discussion, CH_3F has the longest equilibrium *r*(CH) bond in the series of fluorosubstituted methanes: at the MP2(fc)/6-31+G(d,p) level, *r*(CH) = 1.0866 Å, vs 1.0862 Å in CH_4, 1.0859 Å in CH_2F_2, and 1.0849 Å in CHF_3. It is worth mentioning that CH_3F is also characterized by the longest C−F bond, 1.4049 Å (vs 1.3742 Å in CF_2H_2, 1.3502 Å in CF_3H, and 1.3349 Å in CF_4). The C−F stretching frequency is centered at 1057 cm^{-1} (111 km/mol for its IR activity) whereas the C−H stretch is distributed between a mode at 3144 cm^{-1} (33 km/mol) and a doubly degenerate one at 3260 cm^{-1} (27 km/mol).

As mentioned above, the homodimer of this molecule might exist in either a DA structure (**3a**), bound by 2.02 kcal/mol, or one containing a single trifurcated bond (**2e**), bound by 1.47 kcal/mol. Even after ZPVE addition, these complexes are fairly well bound, by 1.36 and 1.20 kcal/mol, respectively. The stability of the latter is attributed in large part to the head-to-tail alignment of dipoles, whereas the former structure contains a less favorable dipole−dipole interaction, which must be supplemented by the relatively strong symmetric H-bonds.

Rotations of the two molecules within cyclic structure **3a** are nearly free: a barrier of only 0.13 kcal/mol is encountered for the rotation of one molecule relative to the other. The relevant transition state involves the interaction of F_2 with both H_8 and H_9. A prior IR study of this complex[52] suggested the presence of the DA geometry in a low-temperature Ar matrix, consistent with our calculations. A recent calculation of the related CH_3I dimer[59] suggests the potential energy surface of the iodine analogue may also contain two minima. The more stable of these two $(CH_3I)_2$ structures bears a certain resemblance to the DA structure **3a** of $(CH_3F)_2$, but the other minimum is quite different from **2e**.

Adding a second F atom to the acceptor yields the DA $CH_3F\cdots CH_2F_2$ structure depicted in Figure 3b and adds 0.54 kcal/mol to the binding energy. CH_2F_2 is a weaker proton acceptor

than CH_3F. The +5.1 mÅ at MP2(fc) (+5.2 mÅ at MP2(full)) stretching of the C_1-F_6 bond and the −1.2 mÅ contraction of C_3-H_{10} are both smaller in magnitude than the corresponding quantities in **3a**. It is hence not surprising that the $F_6\cdots H_{10}$ bond is 2.605 Å longer than the 2.461 Å at MP2(fc) in **3a**. On the other hand, though CH_2F_2 is indeed a weaker proton acceptor than is CH_3F, it is also a stronger donor. Consequently, its *other* H-bond(s), where CH_2F_2 acts as donor, show internal bond length changes that are larger in magnitude. The strength of this bond is amplified at the MP2(full) level, in that the MP2-(fc) $R(F_2\cdots H_{5,7})$ of 2.703 Å is shortened to 2.696 Å at MP2-(full). The presence of the second F atom on CH_2F_2 promotes a greater amount of charge transfer by acting as a sink. Indeed, the C_1-F_4 bond is weakened, as evident by its stretch by 2.1 mÅ [2.3 mÅ at MP2(full)]; shown in magenta in Figure 3b. This minimum is reasonably deep in the sense that switching the particular atoms involved in the H-bonds passes over a barrier of 0.5 kcal/mol; the transition state includes a bifurcated H-bond involving one F and two H's from the other molecule.

The structure retains its DA geometry in $CH_3F\cdots CHF_3$, shown in Figure 3c, and adds another 0.23 kcal/mol to its binding strength. In fact, the $CH_3F\cdots CHF_3$ heterodimer (**3c**) is the most stable dimer among all those examined. Because the dipole moments of its constituents are not arranged in a favorable head-to-tail fashion, its high stability is attributed to the existence of a rather strong $C_3-H_{10}\cdots F_6$ H-bond with the shortest bridge distance $R(F_6\cdots H_{10}) = 2.277$ Å. The relatively strong character of this bond is associated with a high degree of electron transfer from the C_1-F_6 bond to the antibonding σ_{CH}* MO. For CHF_3, the latter MO corresponds to the lowest unoccupied MO (LUMO), localized primarily on the carbon atom.[60] The eigenvalue of this MO corresponds to the lowest $\epsilon_{LUMO} = 1.99$ eV among the various F-substituted methanes. Charge transferred to the CHF_3 molecule is facilitated by C_3-F_4 and C_3-F_5, which act as sinks, associated with their elongation by 1.4 mÅ [1.2 mÅ at MP2(full)].

A secondary, and much less stable, minimum is present on the potential energy surface of this complex, a D structure in Figure 1c containing three bent CH···F bonds. Adding a fourth F atom to the acceptor eliminates the possibility of a cyclic structure, and $CH_3F\cdots CF_4$ is hence limited to the weaker D complexes pictured in Figures 1d and 2f. The former, containing one nonbifurcated CH···F and a second bifurcated CH···F, is energetically roughly equivalent to the latter with its single trifurcated bond.

Higher Degrees of Fluorination. The geometries get somewhat more complicated for higher degrees of fluorination. The potential energy surface of the homodimer of CH_2F_2, for example, contains two separate minima, although both are of the DA variety. The binding energies of these two structures, **3d** and **3e**, are also rather similar. They differ in that the more stable **3e** contains three separate CH···F bonds and the other's arrangement **3d** would be best characterized as two bifurcated bonds. Compared to the former possessing a total dipole moment of 2.86 D, the latter is nonpolar. The greater stability of geometry **3e** is verified by microwave data,[56,57] which conform nicely to that structure. Removing the frozen core approximation from the MP correlation buttresses the case that **3e** is strongly bound in the sense that its $F_6\cdots H_9$ and $F_2\cdots H_7$ distances are shortened by 0.009 Å, and $F_8\cdots H_5$ by 0.006 Å. An earlier computation of this system at the DFT level[34] also found two minima, both of the DA type. The lower minimum is reasonably deep in the sense that its conversion to the same structure, but involving different atoms in the H-bonds, requires some 0.90 kcal/mol. The $CH_2F_2\cdots CHF_3$ complex in Figure 3f is very much like **3e**, containing three separate CH···F bonds and is only slightly weaker overall. A cyclic arrangement is no longer possible for $CH_2F_2\cdots CF_4$, and this complex is limited to a weak, bifurcated bond, pictured in Figure 2g.

Fluoroform Dimer. With regard to trifluorinated CHF_3, its homodimer is able to form a DA structure. (Early ab initio studies[61] of the $CHF_3\cdots CHF_3$ interaction remain uncertain as to whether the most stable geometry is planar[62] or cyclic[63]). As illustrated in Figure 3g, there is some element of bifurcation in the geometry, which is the weakest bound complex of all such DA types. After the present work was originally submitted, another publication appeared dealing with the fluoroform dimer,[64] wherein the intermolecular interaction energies of 14 different orientations were computed via the MP2 method in combination with a variety of basis sets. In particular, one of the chosen geometries (dimer N) corresponds to the experimentally suggested cyclic C_{2h} dimer wherein the two equivalent CH···F H-bonds define a plane, and the remaining F atoms lie in a perpendicular plane. Our full geometry optimizations demonstrate that structure **3g** represents the global minimum on the PES of the fluoroform dimer, and that cyclic structure N corresponds to a transition state of slightly higher energy. Comparison of our structure **3g** with the nonbifurcated geometry proposed by Tsuzuki et al.[64] at the MP2(full)/aug-cc-pvqz level shows the former to be more stable by 0.3 kcal/mol.

In a related matter, it is worth mentioning that very short (H···F) distances of 2.266 and 2.272 Å have been reported for the $F_3CH\cdots FH$ complex at the MP2/6-31+G(d)[50] and MP2/6-311+G(d,p)[48] computational levels, respectively. As shown in more recent work,[65] however, the linear structure of the $F_3CH\cdots FH$ complex, for which these distances pertain, does not represent the global minimum and, in fact, lies some 0.4 (MP2/6-311++G(2d,2p) to 0.6 kcal/mol (MP2/aug-cc-pVTZ) higher in energy. In the true global minimum structure, the CH···F distance is equal to 2.6046 and 2.5757 Å, respectively.

And as a final member of this highly fluorinated family of dimers, $CHF_3\cdots CF_4$ is capable of forming only a single bent CH···F bond, as depicted in Figure 1e.

Changes in Geometry, Frequency, and Charges. The monomers engaging in H-bonded complexes are known to undergo certain interesting changes in their internal geometry. The stretch of the A−H covalent bond in AH···B complexes has been taken as one of the traditional markers of such a bond. More recently it has been revealed that in certain cases, particularly in CH···O bonds, the opposite effect, viz. a C−H bond shortening can occur. The changes suffered by several of the internal bond lengths are indicated in Figures 1−3. The blue numbers refer to changes, in milliangstroms, of those bonds that are directly involved in H-bonds, whereas those of nonparticipating bonds are indicated in magenta.

The data confirm that CH bond shortening is not limited to CH···O bonds, but is also characteristic of CH···F types. The changes are loosely correlated with the strengths of the bonds, in accord with earlier findings.[18] So, for instance, the CH bonds are changed by only very small amounts in Figures 1 and 2 but are larger in Figure 3. This relation between H-bond strength and contraction is illustrated in Figure 4. The weak H-bonds of Figures 1 and 2 are largely clustered in the upper left, as the circles and diamonds, respectively. The data points are scattered with no correlation in evidence, consistent with prior computations.[18] However, the stronger cyclic H-bonds of Figure 3, indicated by the squares, show the clearest correlation. A linear fit, illustrated by the dashed line, has a correlation coefficient

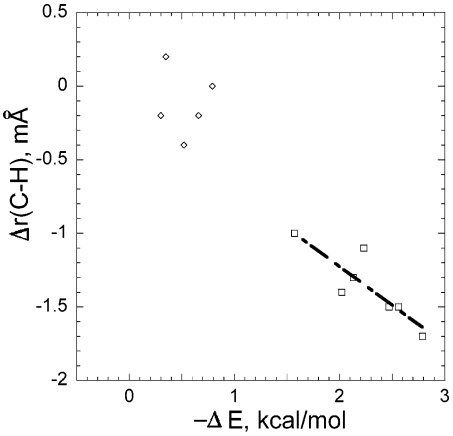

Figure 4. Relation between BSSE-corrected interaction energy and change in C−H bond length. Circles refer to complexes in Figure 1, diamonds to Figure 2, and squares to cyclic complexes in Figure 3. Broken line represents best fit through the latter data set.

of 0.86, and a slope that is consistent with a contraction of some 0.5 mÅ for every 1 kcal/mol of binding energy.

Concomitant with these bond shortenings are blue shifts in their stretching frequencies. Of course, one cannot neatly associate each C−H bond with one and only one normal frequency, as there is a good deal of mixing of C−H bond stretches in many of the normal modes. Nonetheless, it is possible to connect a given stretching mode with at least a select group of CH bonds. First and most definitely, it is obvious that just as nearly all of the bridging CH bonds are shortened, their stretching frequencies are shifted to the blue. The amount of this shift is loosely associated with the degree of bond contraction and with the strength of the interaction binding the two molecules together. For example, these blue shifts range from 0 to 6 cm^{-1} for the generally weak, noncyclic complexes in Figures 1 and 2. The only exception is the particularly strongly bound $CH_3F\cdots CH_3F$ complex **2e**, for which the shift is as large as 13 cm^{-1}.

The shifts are magnified in the stronger, cyclic complexes depicted in Figure 3, which range up to +39 cm^{-1}, as reported in Table 2, together with some selected isotopomers. It is likely no coincidence that the largest such shift occurs for $CH_3F\cdots CHF_3$ complex **3c**, which is the most strongly bound of all complexes considered here, and corresponds to the $\nu(C_3-H_{10})$ stretch of the shortest hydrogen bond $C_3-H_{10}\cdots F_6$. A slightly smaller blue shift of 27 cm^{-1} occurs for the $\nu(C_3-H_9)$ stretch in the $CH_2F_2\cdots CHF_3$ complex **3f**, whose hydrogen bond $C_3-H_9\cdots F_6$ is longer by 0.275 Å, and whose total binding energy is smaller than those of most of the other complexes in Figure 3. Along that line, it should be emphasized that the frequency shifts of the C−H stretch accompanying H-bond formation do not precisely correlate with the interaction energy. As an example, the $CH_3F\cdots CH_2F_2$ complex **3b** is more strongly bound than **3f** (see Table 1 and Figure 3). Yet the former is characterized by a blue shift of 26 (24 for the isotopomer $CH_2DF\cdots CHDF_2$) cm^{-1} for the coupled $\nu(C_1-H_5)$ and $\nu(C_1-H_7)$ stretch (Table 2), which is nearly the same as that in **3f**. It is tempting to speculate, however, about a connection between the large blue shifts in **3c** and **3f**, and the presence of CHF_3, which, as mentioned above, possesses a particularly low-lying LUMO, that facilitates electron transfer. This idea pertains also to the bifurcated H-bonds in the **3b** and **3d** complexes with the corresponding acceptors CHF_3 and CH_2F_2.

It might be noted from Table 2 that the blue frequency shifts are accompanied by a drop in IR intensity, typical of blue-shifting bands. The largest decreases of intensity are predicted for the complexes **3d** and **3a**. Also of some importance, the magnitudes of the frequency and intensity changes are unaffected by expanding the treatment of electron correlation from frozen core to full.

TABLE 2: Blue Shifts ($\Delta\nu$, in cm^{-1}) and Relative IR Activities (ΔI, in km/mol) of C−H Stretching Frequencies of Cyclic Dimers Illustrated in Figure 3.

	MP2(fc)		MP2(full)		
dimer	$\Delta\nu$	ΔI	$\Delta\nu$	ΔI	atoms involved
3a					
$CH_3F\cdots CH_3F$	20	−27			C_1-H_{10}, C_3-H_8
	20	−11			
$CH_2DF\cdots CH_2DF$	17	−21			C_1-D_{10}, C_3-D_8
	17	0			
3b					
$CH_3F\cdots CH_2F_2$	26	−7	26	−7	$C_1-H_{5,7}$
	17	−14	17	−13	C_3-H_{10}
$CH_2DF\cdots CHDF_2$	24	−9			C_1-H_5
	17	−6			C_1-D_7
	13	−9			C_3-D_{10}
3c					
$CH_3F\cdots CHF_3$	39	−20	39	−20	C_3-H_{10}
	16	−12	17	−13	C_1-H_9
$CH_2DF\cdots CDF$	30	−21			C_3-D_{10}
	11	−7			C_1-D_9
3d					
$CH_2F_2\cdots CH_2F_2$	17	−28			$C_1-H_{5,7}$, $C_3-H_{9,10}$
	18	−12			
$CD_2F_2\cdots CH_2F_2$	11	−7			$C_3-D_{9,10}$
	14	−6			
	13	−9			$C_1-H_{5,7}$
	18	−8			
3e					
$CH_2F_2\cdots CH_2F_2$	19	−11	19	−11	C_3-H_9
	20	−12	21	−12	$C_1-H_{5,7}$
$CD_2F_2\cdots CHDF_2$	19	−11			C_3-D_9
	12	−9			$C_1-D_{5,7}$
	16	−9			
3f					
$CH_2F_2\cdots CHF_3$	27	−13			C_3-H_9
	14	−16			$C_1-H_{5,7}$
$CD_2F_2\cdots CHF_3$	27	−13			C_3-H_9
	8	−8			$C_1-D_{5,7}$
	11	−8			
3 g					
$CHF_3\cdots CHF_3$	17	−23			C_1-H_2, C_5-H_4
	17	−3			
$CDF_3\cdots CHF_3$	13	−10			C_1-D_2
	17	−9			C_5-H_4

Even more sensitive to the formation of the CH···F H-bond are the C−F bonds associated with the proton acceptor molecule. These bonds stretch as the CH donor approaches, and again, the degree of change is correlated with H-bond strength. This relationship is presented graphically in Figure 5, where again the dashed line represents the best linear fit of the cyclic H-bonding data in Figure 3. There is a good deal of scatter in the square data points, suggesting caution ought to be used in correlating these stretches with interaction energies.

Table 3 contains the results of a NBO analysis of the three most strongly bound complexes. The results do not fully support the notion that formation of the complex reduces the population of the σ^*(CH) orbital that is involved in each H-bond. On one hand, the pattern in complex **3e** fits this idea, in that the σ^*-(CH) populations of H_5, H_7, and H_9 diminish by some 0.3−0.6. On the other hand, the patterns are less consistent in the other two complexes. For example, this population is reduced by 0.6 for H_5 and H_6 in complex **3b**, but there is a slight *increase* for H_{10}, which is involved in a similar H-bonding interaction. Moreover, even hydrogens not involved in any sort of H-bond

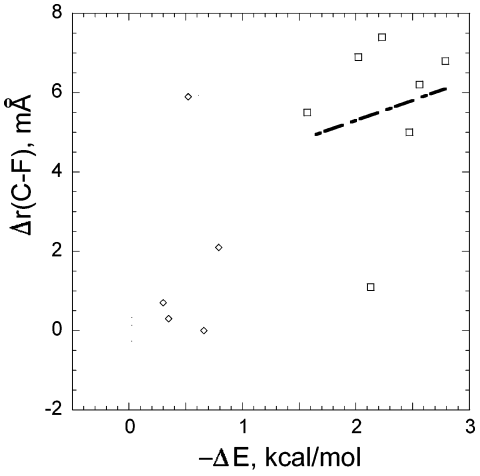

Figure 5. Relation between BSSE-corrected interaction energy and change in C−F bond lengths.

TABLE 3: NBO Analysis of Selected Complexes[a]

complex/atom	Δq	σ^*(CH′)	σ^*(CH″)	σ^*(CF)	LP(F)
		Complex **3b**			
C_1	−0.5				
F_2	−13.6			+0.4	+2.2
C_3	−3.8				
F_4	−4.3			+0.4	−4.2
H_5	+6.5	−0.6			
F_6	−9.2			+0.2	+1.3
H_7	+6.4	−0.6			
H_8	+1.7		−0.6		
H_9	+1.7		−0.6		
H_{10}	+15.1	+0.1			
		Complex **3c**			
C_1	−2.8				
F_2	−9.5			+0.2	+2.9
C_3	−12.7				
F_4	−2.9			−1.3	+1.3
F_5	−2.9			−1.3	+1.3
F_6	−13.4			+0.6	−1.5
H_7	+4.3		−0.8		
H_8	+4.3		−0.8		
H_9	+11.3	−0.3			
H_{10}	+24.3	+0.6			
		Complex **3e**			
C_1	−6.3				
F_2	−4.5			−0.5	+0.3
C_3	−6.0				
F_4	−1.1			−0.7	+0.1
H_5	+7.3	−0.6			
F_6	−11.0			+0.7	+1.8
H_7	+9.8	−0.3			
F_8	−6.5			−0.2	+0.9
H_9	+16.3	−0.6			
H_{10}	+2.0		−0.3		

[a] Quantities reported refer to the difference between the value within the complex and that of the free constituent molecules. Δq (in me) represent atomic charges. σ^*(CH′), σ^*(CH″), and σ^*(CF) correspond to antibonding orbitals of bridging and nonbridging H atoms, respectively, and CF antibonds. The lone pairs of F are represented by LP(F).

at all, e.g., H_8 and H_9, undergo a reduction in their σ^*(CH) population of 0.6. Similar inconsistency is noted in **3c** as well. Although H_9 and H_{10} engage in similar H-bonds in **3c**, the populations of their respective σ^*(CH) orbitals change in different directions. One notes inconsistencies in the F lone pair populations as well. Complex **3b** is well behaved in the sense that F_2 and F_6, both directly engaged in H-bonding, undergo an increase, whereas a decrease is noted in F_4, which is not so engaged. In contrast, F_6 of complex **3c** shows a drop in lone pair population although it is clearly participating in a H-bond.

Conclusions

The potential energy surfaces of the various dimers examined here have a rich landscape, many of them containing more than one minimum. These dimers are held together by CH···F H-bonds. The most strongly bound complexes, with interaction energies in the 2−3 kcal/mol range, are cyclic in nature, wherein each monomer behaves simultaneously as both proton donor and acceptor. The most strongly bound complex of all those considered pairs CH_3F with CHF_3. Noncyclic complexes are only weakly attractive, bound together by less than 0.5 kcal/mol in most cases. Even weaker are bifurcated and trifurcated types of H-bonds, barely bound at all. Every pair of monomers that is in principle capable of forming a cyclic structure does so, and this configuration is always the deepest minimum in the associated potential energy surface.

The covalent CH bonds involved in these CH···F interactions are shortened by formation of the H-bonds, and their stretching frequencies undergo a shift to the blue. As anticipated, the largest such changes are associated with the most strongly bound cyclic complexes. Strongest of all is the cyclic CH_3F···CHF_3 structure **3c**, in which the C−H bond of CHF_3 contracts by 0.0023 Å, and the corresponding stretching frequency increases by 39 cm^{-1}. The C−F bonds, too, are affected by the formation of the CH···F bonds, stretching by even more than their C−H counterparts contract. The largest such change occurs, again, in CH_3F···CHF_3 where the proton-accepting F_6 atom of CH_3F stretches by 0.008 Å away from the C_1 atom and the C_1-F_6 stretching mode undergoes a 20 cm^{-1} red shift. There appears to be some relation between these geometric distortions and the amount of charge transferred from one molecule to the other. In contrast to most earlier predictions, the global minimum of the fluoroform dimer appears to have an unusual structure, which is of general donor−acceptor type, but one of the H-bonds is bifurcated.

Acknowledgment. E.S.K. gratefully thanks Francoise Remacle for warm hospitality and the Region Wallonne (Belgium) for the grant (RW convention 115012). This work was supported financially by NIH grant GM57936 to S. S.

References and Notes

(1) Kobayashi, T.; Hirota, M. *Chem. Lett.* **1972**, 975.
(2) Murray-Rust, P.; Stallings, W. C.; Monti, C. T.; Preston, R. K.; Glusker, J. P. *J. Am. Chem. Soc.* **1983**, *105*, 3206.
(3) Shimoni, L.; Glusker, J. P. *Struct. Chem.* **1994**, *5*, 383.
(4) Howard, J. A. K.; Hoy, V. J.; O'Hagan, D.; Smith, G. T. *Tetrahedron* **1996**, *52*, 12613.
(5) Dunitz, J. D.; Taylor, R. *Chem. Eur. J.* **1997**, *3*, 89.
(6) Desiraju, G. R.; Steiner, T. *The Weak Hydrogen Bond in Structural Chemistry and Biology*; Oxford: New York, 1999.
(7) Barbarich, T. J.; Rithner, C. D.; Miller, S. M.; Anderson, O. P.; Strauss, S. H. *J. Am. Chem. Soc.* **1999**, *121*, 4280.
(8) Allerhand, A.; Schleyer, P. v. R. *J. Am. Chem. Soc.* **1963**, *85*, 1715.
(9) Creswell, C. J.; Allred, A. L. *J. Am. Chem. Soc.* **1963**, *85*, 1723.
(10) Hobza, P.; Havlas, Z. *Chem. Phys. Lett.* **1999**, *303*, 447.
(11) Alkorta, I.; Rozas, I.; Elguero, J. *J. Fluorine Chem.* **2000**, *101*, 233.
(12) Reimann, B.; Buchhold, K.; Vaupel, S.; Brutschy, B.; Havlas, Z.; Spirko, V.; Hobza, P. *J. Phys. Chem. A* **2001**, *105*, 5560.
(13) van der Veken, B.; Herrebout, W. A.; Szostak, R.; Shchepkin, D. N.; Havlas, Z.; Hobza, P. *J. Am. Chem. Soc.* **2001**, *123*, 12290.
(14) Sosa, G. L.; Peruchena, N. M.; Contreras, R. H.; Castro, E. A. *J. Mol. Struct. (THEOCHEM)* **2002**, *577*, 219.
(15) Delanoye, S. N.; Herrebout, W. A.; van der Veken, B. J. *J. Am. Chem. Soc.* **2002**, *124*, 7490.
(16) Delanoye, S. N.; Herrebout, W. A.; van der Veken, B. J. *J. Am. Chem. Soc.* **2002**, *124*, 11854.

(17) Melikova, S. M.; Rutkowski, K. S.; Rodziewicz, P.; Koll, A. *Chem. Phys. Lett.* **2002**, *352*, 301.
(18) Kryachko, E. S.; Zeegers-Huyskens, T. *J. Phys. Chem. A* **2001**, *105*, 7118.
(19) Pejov, L.; Hermansson, K. *J. Chem. Phys.* **2003**, *119*, 313.
(20) Steiner, T. *Chem. Commun.* **1997**, 727.
(21) Scheiner, S. *Hydrogen Bonding: A Theoretical Perspective*; Oxford University Press: New York, 1997.
(22) Gu, Y.; Kar, T.; Scheiner, S. *J. Am. Chem. Soc.* **1999**, *121*, 9411.
(23) Scheiner, S. CH···O Hydrogen Bonding. In *Advances in Molecular Structure Research*; Hargittai, M., Hargittai, I., Eds.; JAI Press: Stamford, CT, 2000; Vol. 6; p 159.
(24) Steiner, T. *Angew. Chem., Int. Ed. Engl.* **2002**, *41*, 48.
(25) Hobza, P.; Havlas, Z. *Theor. Chem. Acc.* **2002**, *108*, 325.
(26) Kryachko, E. S.; Zeegers-Huyskens, T. *J. Phys. Chem. A* **2002**, *106*, 6832.
(27) Wiechert, D.; Mootz, D.; Dahlems, T. *J. Am. Chem. Soc.* **1997**, *119*, 12665.
(28) Thalladi, V. R.; Weiss, H.-C.; Bläser, D.; Boese, R.; Nangia, A.; Desiraju, G. R. *J. Am. Chem. Soc.* **1998**, *120*, 8702.
(29) Lee, H.; Knobler, C. B.; Hawthorne, M. F. *Chem. Commun.* **2000**, 2485.
(30) Desiraju, G. R. *Acc. Chem. Res.* **2002**, *35*, 565.
(31) Vangala, V. R.; Nangia, A.; Lynch, V. M. *Chem. Commun.* **2002**, 1304.
(32) Mountford, A. J.; Hughes, D. L.; Lancaster, S. J. *Chem. Commun.* **2003**, 2148.
(33) Weiss, H.-C.; Boese, R.; Smith, H. L.; Haley, M. M. *Chem. Commun.* **1997**, 2403.
(34) Cabral, B. J. C.; Guedes, R. C.; Pai-Panandiker, R. S.; de Castro, P. A. N. *Phys. Chem. Chem. Phys.* **2001**, *3*, 4200.
(35) Cole, G. C.; Legon, A. C. *Chem. Phys. Lett.* **2003**, *369*, 31.
(36) Wang, X.; Houk, K. N. *Chem. Commun.* **1998**, 2631.
(37) Santhosh, C.; Mishra, P. C. *Int. J. Quantum Chem.* **1998**, *68*, 351.
(38) Barsky, D.; Kool, E. T.; Colvin, M. E. *J. Biomol. Struct. Dynam.* **1999**, *16*, 1119.
(39) Bats, J. W.; Parsch, J.; Engels, J. W. *Acta Crystallogr., Sect.C: Cryst. Struct. Commun.* **2000**, *C56*, 201.
(40) Parsch, J.; Engels, J. W. *J. Am. Chem. Soc.* **2002**, *124*, 5664.
(41) Karger, N.; Amorim da Costa, A. M.; Ribeiro-Claro, J. A. *J. Phys. Chem. A* **1999**, *103*, 8672.
(42) Marques, M. P. M.; da Costa, A. M. A.; Ribeiro-Claro, P. J. A. *J. Phys. Chem. A* **2001**, *105*, 5292.
(43) Wetmore, S. D.; Schofield, R.; Smith, D. M.; Radom, L. *J. Phys. Chem. A* **2001**, *105*, 8718.
(44) Mizuno, K.; Imafuji, S.; Fujiwara, T.; Ohta, T.; Tamiya, Y. *J. Phys. Chem. B* **2003**, *107*, 3972.
(45) Masunov, A.; Dannenberg, J. J.; Contreras, R. H. *J. Phys. Chem. A* **2001**, *105*, 4737.
(46) Hermansson, K. *J. Phys. Chem. A* **2002**, *106*, 4695.
(47) Kovác, A.; Szabó, A.; Nemcsok, D.; Hargittai, I. *J. Phys. Chem. A* **2002**, *106*, 5671.
(48) Li, X.; Liu, L.; Schlegel, H. B. *J. Am. Chem. Soc.* **2002**, *124*, 9639.
(49) Qian, W.; Krimm, S. *J. Phys. Chem. A* **2002**, *106*, 11663.
(50) Alabugin, I. V.; Manoharan, M.; Peabody, S.; Weinhold, F. *J. Am. Chem. Soc.* **2003**, *125*, 5973.
(51) Frisch, M. J.; Trucks, G. W.; Schlegel, H. B.; Scuseria, G. E.; Robb, M. A.; Cheeseman, J. R.; Zakrzewski, V. G.; Montgomery, J. A.; Stratmann, R. E.; Burant, J. C.; Dapprich, S.; Millam, J. M.; Daniels, A. D.; Kudin, K. N.; Strain, M. C.; Farkas, O.; Tomasi, J.; Barone, V.; Cossi, M.; Cammi, R.; Mennucci, B.; Pomelli, C.; Adamo, C.; Clifford, S.; Ochterski, J.; Petersson, G. A.; Ayala, P. Y.; Cui, Q.; Morokuma, K.; Malick, D. K.; Rabuck, A. D.; Raghavachari, K.; Foresman, J. B.; Cioslowski, J.; Ortiz, J. V.; Stefanov, B. B.; Liu, G.; Liashenko, A.; Piskorz, P.; Komaromi, I.; Gomperts, R.; Martin, R. L.; Fox, D. J.; Keith, T.; Al-Laham, M. A.; Peng, C. Y.; Nanayakkara, A.; Gonzalez, C.; Challacombe, M.; Gill, P. M. W.; Johnson, B.; Chen, W.; Wong, M. W.; Andres, J. L.; Gonzalez, C.; Head-Gordon, M.; Replogle, E. S.; Pople, J. A. *Gaussian 98*, revision A.7; Gaussian Inc.: Pittsburgh, PA, 1998.
(52) Futami, Y.; Kudoh, S.; Takayanagi, M.; Nakata, M. *Chem. Phys. Lett.* **2002**, *357*, 209.
(53) Graul, S. T.; Squires, R. R. *J. Am. Chem. Soc.* **1990**, *112*, 2517.
(54) Lee, E. P. F.; Dyke, J. M.; Mayhew, C. A. *J. Phys. Chem. A* **1998**, *102*, 8349.
(55) Deyerl, H.-J.; Alconcel, L. S.; Continetti, R. E. *J. Phys. Chem. A* **2001**, *105*, 552.
(56) Caminati, W.; Melandri, S.; Moreschini, P.; Favero, P. G. *Angew. Chem., Int. Ed. Engl.* **1999**, *38*, 2924.
(57) Blanco, S.; Lopez, J. C.; Lesarri, A.; Alonso, J. L. *J. Mol. Struct.* **2002**, *612*, 255.
(58) Monat, J. E.; Toczylowski, R. R.; Cybulski, S. M. *J. Phys. Chem. A* **2001**, *105*, 9004.
(59) Bogdanchikov, G. A.; Baklanov, A. V.; Parker, D. H. *Chem. Phys. Lett.* **2003**, *376*, 395.
(60) Modelli, A.; Scagnolari, F.; Distefano, G.; Jones, D.; Guerra, M. *J. Chem. Phys.* **1992**, *96*, 2061.
(61) Palmer, B. J.; Anchell, J. L. *J. Phys. Chem.* **1995**, *99*, 12239.
(62) Popowicz, A.; Ishida, T. *Chem. Phys. Lett.* **1981**, *83*, 520.
(63) Buckingham, A. D.; Raab, R. E. *J. Chem. Soc.* **1961**, 5511.
(64) Tsuzuki, S.; Uchimaru, T.; Mikami, M.; Urata, S. *J. Phys. Chem. A* **2003**, *107*, 7962.
(65) Karpfen, A.; Kryachko, E. S. *J. Phys. Chem. A* **2003**, *107*, 9724.